SEAMLESS MULTISCALE MODELING OF COMPLEX FLUIDS USING FIBER BUNDLE DYNAMICS *

WEIQING REN †

Abstract. We present a seamless multiscale model and an efficient coupling scheme for the study of complex fluids. The multiscale model consists of macroscale conservation laws for mass and momentum, molecular dynamics on fiber bundles, as well as the Irving-Kirkwood formula which links the macroscale stress tensor with the microscopic variables. The macroscale and microscale models are solved with a macro time step and a micro time step respectively. The two models are synchronized at each time step by exchanging the velocity gradient (from macro to micro) and the stress tensor (from micro to macro). The multiscale method is applied to study the dynamics of polymer fluids in a channel driven by external forces.

Key words. multiscale modeling; complex fluids; molecular dynamics; fiber bundle

AMS subject classifications. 76M25; 65C35; 65Z05

1. Introduction

The modeling of constitutive equations for the stress tensor represents one of the major difficulties in the study of macroscale behaviors of complex fluids. For simple fluids, the simple linear relation between the stress and the strain rate, with all molecular details lumped into a single parameter, i.e. the viscosity, works remarkably well. For complex fluids such as polymers or liquid crystals, however, the constitutive relation becomes much more complicated, essentially due to the complex nature of constituting molecules. Conventionally, this relation has been modeled empirically in these situations. In recent years, there has been a growing interest on modeling this relation using first-principle microscale models, such as Brownian dynamics [1] or molecular dynamics (MD) [2]. The stress which is either pre-computed or calculated "on the fly" from a microscale model is used to solve the macroscale conservation laws to capture the macroscopic behavior of the system. This kind of multiscale model bypasses the necessity for making ad hoc modeling assumptions; thus in principle it has the accuracy of the microscopic model, while retaining much of the efficiency of a continuum model.

In this paper, we introduce a seamless multiscale method for the study of complex fluids. The multiscale model is built upon a general framework proposed in Ref. [3], and it is formulated using microscopic dynamics on fiber bundles. The fibers are associated with the physical domain of interest. The macroscale dynamics of the fluid is described by the conservation laws of mass and momentum over the physical domain, in the meanwhile the stress tensor is computed from molecular dynamics over the fibers "on the fly". Therefore, our multiscale model contains a system of coupled equations, including the macroscale conservation laws and the microscale molecular dynamics. The two models are solved using different time steps - one is of macroscopic scale and the other is of microscopic scale. The two models are synchronized at each macro and micro time step by exchanging data. The main advantage of this multiscale model is that the macro and micro dynamics are coupled seamlessly, and it avoids the need for explicitly going back and forth between these two models. In contrast, the method we proposed earlier in Ref. [2] requires going back and forth explicitly

*

†Courant Institute of Mathematical Sciences, New York University, New York, NY 10012, USA, (weiqing@cims.nyu.edu).

between the macro and micro models, thus it is not seamless. In particular, the method in Ref. [2] has the drawback that one needs to reinitialize MD each time when the stress is needed.

In the following we describe the structure of the multiscale model and the numerical scheme for solving this model. We will present two numerical examples, in which the multiscale method is applied to study the dynamics of channel flows which are driven external forces.

2. The Multiscale Method

2.1. Formulation of the multiscale model. Let us denote the spatial domain of interest by Ω. We associate with Ω a collection of fibers $\{\gamma_x,\ x\in\Omega\}$. Our multiscale model consists of three components: A macroscale dynamics on Ω, a microscale dynamics on γ_x, and a link between these two dynamics. The link specifies the model input for the macro dynamics using the microscale model. Next we discuss these three components in details.

Our macroscale model for the fluid system is the conservation of mass and momentum:

$$\begin{cases} \rho(\partial_t u+\nabla\cdot(u\otimes u))-\nabla_x\cdot\tau=0, \quad x\in\Omega \\ \nabla\cdot u=0 \end{cases} \tag{2.1}$$

where ρ, u and τ are the fluid density, the velocity field and the stress tensor respectively. At this level, the system is not closed since the stress tensor is yet to be specified. In the multiscale method, the stress is calculated from a microscale model as described below.

Our microscale model for the stress tensor is molecular dynamics of N particles in each fiber γ_x, where $\gamma_x=\{1,2,\cdots,N\}$ and the integers are the indices of the particles. These particles evolve in time according to Newton's equation:

$$m_i\ddot{r}_i=f_i, \quad i=1,2,\cdots,N \tag{2.2}$$

where m_i and r_i are the particle mass and position respectively, f_i is the atomistic force on the i-th particle. The MD in each fiber is conducted in a finite box; the volume of the box is determined by the particle number N and the particle density ρ. Here we assume the stress tensor only depends on the velocity gradient $A(x,t)=\nabla_x u$, where u is the macroscale velocity field. Then the MD systems have to be constrained so that at time t the mean velocity gradient in the fiber γ_x is equal to $A(x,t)$. This constraint is imposed through the boundary condition which will be discussed later in the numerical examples.

The macroscale model (2.1) and the microscale model (2.2) are linked together through the Irving-Kirkwood formula [4], which expresses the stress tensor in terms of the microscale variables. Specifically, the macroscale stress tensor at (x,t) is computed from MD in the corresponding fiber γ_x and at the time t:

$$\begin{aligned} \tilde{\tau}(\xi,t;x)=&-\sum_i(m_i v_i\otimes v_i)\delta(r_i-\xi) \\ &-\frac{1}{2}\sum_{j\neq i}((r_i-r_j)\otimes f_{ij})\int_0^1\delta(\lambda r_i+(1-\lambda)r_j-\xi)\,d\lambda, \end{aligned} \tag{2.3}$$

where $v_i=\dot{r}_i-Ar_i$ is the thermal velocity of the i-th particle, and f_{ij} is the force acting on the i-th particle by the j-th particle. The average of $\tilde{\tau}$ over the MD simulation

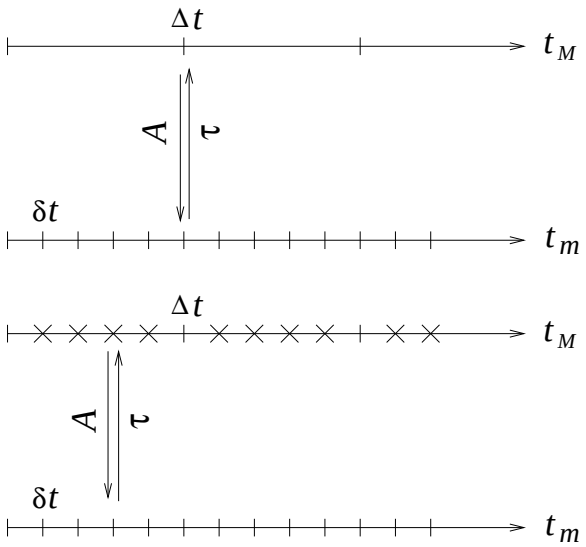

FIG. 2.1. *Two strategies for the coupling of the macro and micro models. Upper panel: The macro and micro dynamics are solved with a macro time step Δt and a micro time step δt respectively; the two models exchange data at every macro time step and every M micro steps. Lower panel: The macro dynamics is solved using a reduced macro time step $\Delta t/M$; the two models exchange data at every (reduced) macro and micro time step.*

box ω gives the stress needed in the macro model:

$$\tau(x,t) = \frac{1}{V}\int_{\omega} \tilde{\tau}(\xi,t;x)d\xi. \tag{2.4}$$

where V is the volume of ω.

Equations (2.1), (2.2) and (2.3), (2.4) form our multiscale model. Equation (2.1) is the macroscale model for the velocity field, Eq. (2.2) is the microscale model in the fibers γ_x. Eqs. (2.3) and (2.4) provides the stress tensor and give the link between the two models.

2.2. Coupling scheme. The macro and micro models in Eqs. (2.1) and (2.2) contain at least two disparate time scales: A macro scale associated with the hydrodynamics, and a micro scale associated with the fast molecular motions. This gives rise to the following difficulty when numerically solving the coupled models: On one hand we are interested in the macroscale hydrodynamics, on the other hand, we are forced to use a time step δt which is of microscopic size in order to resolve the fast molecular motions in MD. It would be prohibitively expensive to solve the coupled models simultaneously over a hydrodynamics time scale.

This difficulty can be overcome using the fact that the particle system relaxes to a (quasi) steady state on a microscopic time scale; consequently the MD constrained by the velocity gradient at every macro time step reaches the steady state after M micro steps, where $M\delta t \ll \Delta t$, Δt and δt are the macro and micro step size respectively. This suggest the following numerical scheme: Solve the macro dynamics with a macro step size Δt; at the same time solve the constrained MD for M steps with a micro step size δt, and then synchronize the two models by exchanging the velocity gradient and the stress. This procedure is illustrated in the upper panel of Fig. 2.1.

A more efficient coupling scheme is to synchronize the two models at each micro step. This requires solving the macro dynamics using a reduced time step $\Delta t' = \Delta t/M$. This procedure is illustrated in the lower panel of Fig. 2.1. By exchanging data at every macro and micro time step, the data calculated from the micro model are implicitly averaged over time, and the resulting data contain less statistical errors. To see this let us assume the macroscale variable is x and it is governed by the equation $\dot{x} = f(x,y)$. Here y is a fast variable and is supplied by some microscale model. We now solve this equation for x using the simplest solver, the forward Euler, with a time step $\Delta t/M$:

$$x^{k+1} = x^k + \frac{\Delta t}{M} f(x^k, y^k), \quad k = 0,1,\cdots \tag{2.5}$$

where x^k is the numerical solution at $t_M^k = k\Delta t/M$, and y^k is the numerical solution to the micro model at $t_m^k = k\delta t$. From (2.5) it is easy to see that the numerical solution of x at $t_M^k + \Delta t$ can be expressed as

$$x^{k+M} = x^k + \Delta t F^k \tag{2.6}$$

where $F^k = M^{-1} \sum_{i=k}^{k+M-1} f(x^i, y^i)$ is the average of f over the previous M steps.

The procedure of solving the coupled macro and micro models is summarized in the following:

(0) Prepare the initial data for the macro and micro models; choose the parameter M, which is the number of micro steps conducted per macro time interval Δt;
(1) Solve the macro and micro models using standard solvers for one time step with step size $\Delta t' = \Delta t/M$ and δt respectively;
(2) Synchronize the two models by exchanging data;
(3) Go to step (1).

The above algorithm is equivalent to rescaling the micro dynamics according to $t \to \zeta t$, where $\zeta = M\delta t/\Delta t$, then solving the macro and the rescaled micro models with the same time step $\Delta t/M$. The idea of rescaling the fast dynamics has been used before in boosting algorithms. In boosting algorithms, the small parameter present in the original micro model is replaced by a larger, boosted value, and the resulting modified equations are solved by standard solvers. This kind of ideas have been used in Chorin's artificial compressibility method [5] and Car-Parrinello *ab initio* molecular dynamics [6]. It was recently discussed in a general context in [7]. The algorithm presented here is different from the boosting algorithms in the following aspect: In the method based on fiber bundle dynamics, one solves the coupled macroscale (effective) and microscale equations; the macroscale (slow) variables have to be identified and the macroscale model needs to be formulated beforehand. In contrast, in boosting algorithms only the modified micro-model is solved and one does not need to identify the slow variables beforehand. Further discussions and comparisons of these methods will be presented in [8].

3. Applications of the Multiscale Method

We next discuss the implementation issues of the multiscale method and demonstrate its efficiency by two examples.

3.1. Problem setup. We calculate the dynamics of a channel flow driven by an external force, as illustrated in Fig. 3.1. We will consider two types of fluids

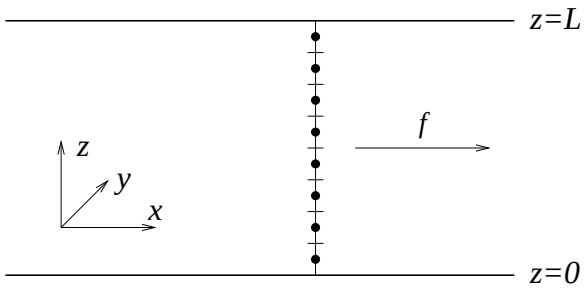

FIG. 3.1. *Schematic illustration of the system studied in the numerical example and the computational mesh for the macroscale model. The velocity is defined at the grid point, and the shear stress is defined at the center of each cell indicated by black dots.*

respectively. In the first example the fluid consists of Lennard-Jones particles, and in the second example the fluid consists of polymers. The first example serves as a benchmark for the multiscale method, whose solution will be compared with the solution of the Navier-Stokes equation.

The flow is driven by a time-dependent external force $f(t)$ in x-direction. Since the flow is homogeneous in both x and y directions, the macroscale model (2.1) reduces to

$$\rho\partial_t u = \partial_z \tau + f(t), \quad 0 < z < L \tag{3.1}$$

where u is the velocity in the x-direction and τ is the shear stress. Equation (3.1) is supplemented with initial condition $u = 0$ and the no-slip boundary condition $u = 0$ at the two channel walls located at $z = 0$ and $z = L$ respectively.

The spatial domain $[0, L]$ is covered by a uniform mesh $\{z_i = i\Delta z, i = 0, 1, \cdots, I\}$, where $\Delta z = L/I$ is the mesh size. Equation (3.1) is discretized by the forward Euler method in time and central difference in space:

$$\rho\frac{u_i^{k+1} - u_i^k}{\Delta t'} = \frac{\tau_{i+1/2}^k - \tau_{i-1/2}^k}{\Delta z} + f^k, \quad \begin{array}{l} i = 1, 2, \cdots, I-1 \\ k = 0, 1, 2, \cdots \end{array} \tag{3.2}$$

where u_i^k is the velocity at the grid point z_i and at time $t_k = k\Delta t'$, $\Delta t' = \Delta t/M$ is the macro time step; $\tau_{i+1/2}^k$ is the shear stress defined at $z_{i+1/2}$ which is the center of the cell $[z_i, z_{i+1}]$; f^k is the driving force at t_k. The difference equation is supplemented with the initial and boundary conditions:

$$u_i^0 = 0, \quad u_0^k = u_I^k = 0. \tag{3.3}$$

Corresponding to the discretized spatial domain, we have I fibers, $\{\gamma_{i+1/2}, i = 0, 1, \cdots, I-1\}$, each of which is associated with one cell. The Newton's equation (2.2) is solved in each of these fibers and provides the shear stress $\tau_{i+1/2}^k$. Each MD is constrained by the velocity gradient in the corresponding cell. The velocity gradient is calculated using finite difference:

$$A_{i+1/2}^k = \frac{u_{i+1}^k - u_i^k}{\Delta z}, \quad i = 0, 1, \cdots, I-1. \tag{3.4}$$

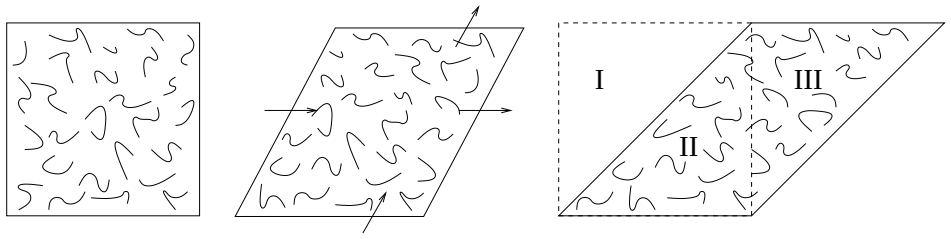

FIG. 3.2. *Schematic illustration of the constrained MD simulation. The MD box deforms according to the specified velocity gradient. Periodic boundary condition for particle positions is applied on the deforming box. The left panel shows the initial configuration; the middle and right panels show the configuration at two later times. When the box vertices coincide with the lattice defined by the initial box, the simulation is reinitialized by shifting the molecules in the region III to the region I.*

Note that A in this example is a scalar and denotes the shear rate.

Each MD system contains N particles in a 3d simulation box. The interaction potential between the particles will be specified later. The Newton's equation is solved using the velocity Verlet algorithm, with a micro time step δt. The technique of cell list is used to reduce the computational cost. The dynamic equation in the y-direction (span-wise direction) is modified by adding a noise term and a damping term in order to control the temperature.

Imposing constraints on MD represents the major difficulty in the multiscale method. For the system considered here, we need to impose a given shear rate and this is done by applying the Lees-Edwards boundary condition [9, 2] (see Fig. 3.2). The left panel in Fig. 3.2 shows the initial configuration of the MD system. As the simulation proceeds, the MD box deforms its shape based on the specified shear rate A. Denote the coordinates of the box vertices by $\{(X_j, Y_j, Z_j), j = 1, 2, \cdots, 8\}$, then the dynamics of the box is governed by:

$$\dot{X}_j = AZ_j, \quad \dot{Y}_j = \dot{Z}_j = 0. \tag{3.5}$$

The middle panel of the figure shows a snapshot of the deforming box. At the time when the vertices of the deforming box coincide with the vertices of the lattice defined by the initial box, as shown in the right panel of Fig. 3.2, we reinitialize the simulation by periodically shifting the particles back to the initial box. Note that this reinitialization does not change the configuration of the system. Periodic boundary condition for particle positions is applied on the deforming box, that is, when a particle crosses a boundary, we put it back into the box from the opposite side, and at the same time modify its velocity according to the imposed velocity gradient. This is illustrated in the middle panel of Fig. 3.2.

We summarize the computation procedure in the following algorithm:

(0). Given the initial velocity $\{u_i^0 = 0, i = 0, 1, \cdots, I\}$, and initial configuration of the MD system in each fiber, let $k = 0$;
(1). Compute the shear rates $\{A_{i+1/2}^k, i = 0, 1, \cdots, I-1\}$ according to Eq. (3.4);
(2). Solve the MD systems for one step with step size δt, and compute the shear stress $\tau_{i+1/2}^k$ using the Irving-Kirkwood formula. The MD in $\gamma_{i+1/2}$ is constrained by $A_{i+1/2}^k$;

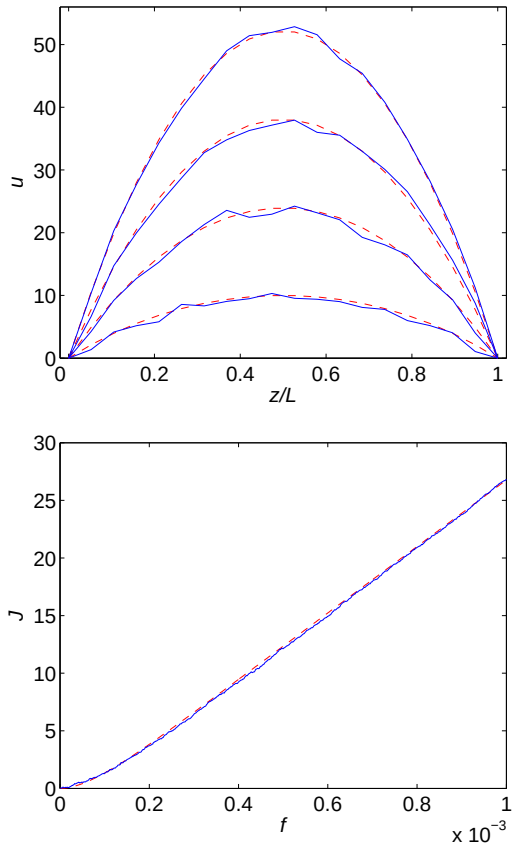

FIG. 3.3. *Numerical results for the LJ fluid. Solid curves are numerical solutions to the multiscale model; dashed curves are the solutions to the Navier-Stokes equation. The upper panel shows the velocity profile at different times:* $t = 1.25\times10^5, 2.5\times10^5, 3.75\times10^5$ *and* 5×10^5 *from the bottom to the top respectively. The lower panel shows the mass flux density as a function of the driving force.*

(3). Using Eq. (3.2) and the stresses calculated in step (2), solve the macroscale model for one step with step size $\Delta t' = \Delta t/M$ to get u_i^{k+1};
(4). Let $k := k+1$ and go to step (1).

The parameters Δt and δt should be chosen according to the timescale of the hydrodynamics and the fast molecular motions, respectively. The parameter M, which is the number of MD steps conducted per macro time interval Δt, depends on the molecular relaxation time. Further discussions on the choice of M will be given in the last section.

3.2. Application to a simple fluid. In this example, the fluid consists of particles of equal mass m interacting via the Lennard-Jones (LJ) potential:

$$V^{LJ}(r) = 4\epsilon\left(\left(\frac{\sigma}{r}\right)^{12} - \left(\frac{\sigma^6}{r}\right)\right) \tag{3.6}$$

where r is the distance between particles, ϵ and σ are characteristic energy and length scales. In the following, we express all physical quantities in these atomic units, e.g. the unit of length is σ, the unit of time is $\sigma\sqrt{m/\epsilon}$, the unit of density is m/σ^3, the unit of temperature is ϵ/k_B where k_B is the Boltzmann constant, and etc.

The size of the channel is $L=10^3$. The external force is $f(t)=2\times10^{-9}t$. The spatial domain is discretized into $I=19$ cells. The macro time step is $\Delta t'=\Delta t/M$ where $\Delta t=500$ and $M=40$. The parameters used in the MD systems are as follows: Each MD system contains $N=9072$ particles; the initial simulation box has the dimension $115.6\times7.51\times12.87$; the particle density is $\rho=0.81$; the temperature is $T=1.1$; the micro time step is $\delta t=0.005$.

The numerical results are shown in Fig. 3.3. The upper panel shows the snapshot of the velocity profile at several different times (solid curves). The lower panel shows $J=L^{-1}\int_0^L \rho u dz$, the averaged mass flux density across the channel, as a function of the driving force f. The small wiggles in the velocity profiles are due to statistical errors in the measured stress, which can be reduced by increasing the size of the MD system, and/or by using a larger value of M.

For simple LJ fluids, the Navier-Stokes (NS) equation, in which the stress is modeled by the linear constitutive equation, is an accurate model for describing the dynamics. For the channel flow considered in this example, the NS equation reduces to

$$\rho\partial_t u=\mu\partial_z^2 u+f(t) \tag{3.7}$$

where $\rho=0.81$ and $\mu=2.0$ corresponding to our MD system. The solution to this continuum equation is shown in Fig. 3.3 as the dashed curves. They are in good agreement with the results of the multiscale method.

3.3. Application to a polymer fluid. Next we consider polymer fluids. At molecular scale, the polymers are modeled by the bead-spring model: Each polymer consists of m beads, neighboring beads are connected by a spring force which is modeled by the FENE potential:

$$V^{FENE}(r)=\begin{cases}\frac{1}{2}kr_0^2\ln\left(1-\left(\frac{r}{r_0}\right)^2\right), & r<r_0,\\ \infty, & r\geq r_0\end{cases} \tag{3.8}$$

where $k=30$ and $r_0=1.5$. To prevent the beads from overlapping, the LJ potential is added to the interactions among all beads.

The size of the channel, the driving force and Δt remain the same as before. Since the polymers have a larger relaxation time than LJ particles, we used a larger value for M: $M=200$. Each MD system contains $N_p=800$ polymers. Each polymer has $m=12$ beads of the same mass. The initial simulation box has the dimension $45.6\times22.8\times11.4$. The density of beads is $\rho=0.81$. The temperature is $T=1.1$. The MD time step is $\delta t=0.002$.

The numerical solutions to the multiscale model are shown in Fig. 3.4. The upper panel shows the velocity profiles at different times. The solid curves are obtained using the algorithm in which the macro model is solved with the reduced step size $\Delta t'=\Delta t/M$ and it exchanges data with the micro model at every time step; the dashed curves are obtained using the scheme in which the macro model is solved with the time step Δt and it exchanges data with the micro model for every M micro steps. These two schemes are illustrated in Fig. 2.1. As we expected, the results obtained

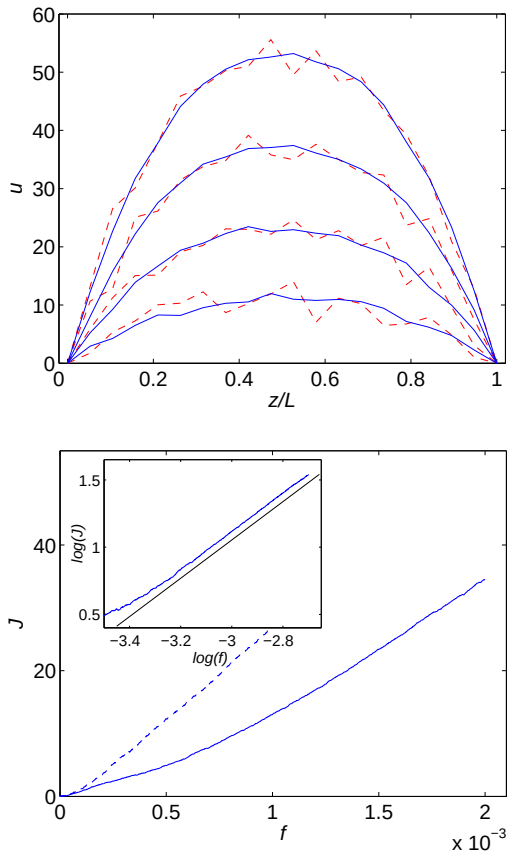

FIG. 3.4. *Numerical results for the polymer fluid. Upper panel: the velocity profile at different times:* $t = 3\times10^5, 5\times10^5, 7\times10^5$ *and* 9×10^5 *from the bottom to the top respectively. The solid and dashed curves are obtained by using a macro time step* $\Delta t' = \Delta t/M$ *and* Δt *respectively. Lower panel: the mass flux density as a function of the driving force. For comparison, the mass flux density for the LJ fluid is also shown here (the dashed curve). Inset: A* log-log *plot of the mass flux density versus the driving force. A straight line of slope 1.42 is drawn for eye guidance.*

using the reduced time step are much smoother. This is due to the fact that the data calculated from MD are implicitly averaged over time, thus contain less statistical errors.

The lower panel shows the averaged mass flux density as a function of the external force. For comparison, the mass flux density obtained in the previous example for LJ fluids is also shown (the dashed curve). The inset shows a log-log plot of the mass flux of the polymer fluid versus the driving force. A straight line of slope 1.42 is drawn for eye guidance. The logarithm of the mass flux follows closely this straight line, which indicates the mass flux increases super-linearly with increasing driving force: $J \propto f^{1.42}$. This is a consequence of the shear-thinning property of polymer fluids, and is in contrast to simple fluids where the mass flux is a linear function of f.

4. Concluding Remarks

The choice of the parameter M is important to the success of the multiscale

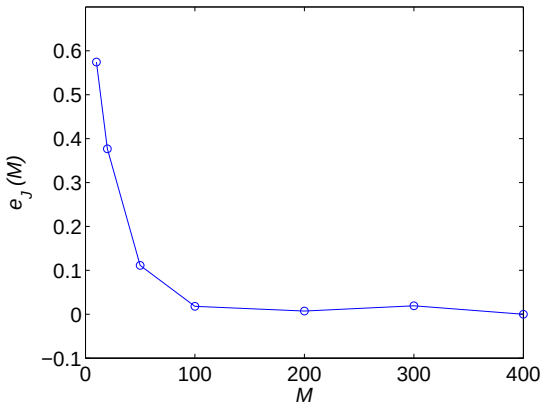

FIG. 4.1. *Relative error of the computed mass flux of polymer fluids at* $t = 2.7 \times 10^5$ *versus* M, *the number of MD steps per macro time interval* Δt.

method. This parameter should be chosen such that $M\delta t$ is larger than the molecular relaxation time. Figure 4.1 shows the dependence of the accuracy of the numerical results on the choice of M. In this figure we plot the relative error of the computed mass flux of the polymer fluids as a function of M. The error is defined as $e_J(M) = |J(M) - J_\infty|/J_\infty$, where J_∞ is the mass flux density calculated using a large M: $M = 400$. As expected, the error decreases as M is increased and it levels off when $M \geq 100$. Therefore, for this system we need to conduct at least $M^* = 100$ MD steps per macro time interval Δt in order to obtain accurate results. The computational cost increases linearly with M.

In the multiscale model formulated in this paper, the stress needed in the macro model is computed from MD "on the fly" as the computation proceeds. This is an example of the concurrent coupling methods. An alternative is to use the sequential coupling strategy, in which the constitutive relation is computed from MD beforehand, then one solves the effectively closed macroscale model. This latter approach requires pre-computing the full constitutive equation and is thus very often too expensive, especially for problems in high dimensions where the constitutive relation depends on many variables. In contrast, in concurrent coupling methods, one does not compute the constitutive relation within the full range of these variables - only the values that actually occur in the simulation are needed, and these might be a very small subset of the entire range. Nevertheless, we would point out that the sequential coupling strategy can still be made efficient even in situations when the constitutive relation depends on many variables. But this requires more sophisticated techniques [10].

In this paper, we focused on the strategy for coupling the macroscale and microscale models. Another important issue in such a multiscale method is the imposition of constraints on molecular dynamics. In our numerical examples, the constraint (shear rate) was imposed by applying the periodic boundary condition on a deforming MD box. When applied to 2d or 3d flows, this technique has the following difficulty: the MD box deforms exponentially fast, and the simulation breaks down when the box size in certain direction decreases to the molecular interaction scale. This issue is partially resolved for 2d time-independent problems [11, 12]. The resolution rests on a clever choice of the initial simulation box. However, this kind of methods can not

be applied to simulate 3d flows or impose time-dependent velocity gradients. These problems will be studied in the future work.

In this paper, we considered the modeling of constitutive relations using MD on fiber bundles. For problems with complex fluid-solid interactions or chemical reactions, the conventionally used no-slip boundary condition becomes inaccurate. In this situation, one can formulate and use a multiscale model to study the macroscale behavior of the system, in a similar way as we did in this paper for complex fluids. In the multiscale model, the boundary conditions will be computed from an atomistic model, such as molecular dynamics.

Acknowledgement. The author is grateful to Weinan E, Eric Vanden-Eijnden, Bob Kohn and Jianfeng Lu for very helpful discussions. The author thanks Eric Vanden-Eijnden for bringing to his attention Ref. [13], where ideas similar to the implicit time-averaging using a reduced macro time step were used. This work is partially supported by NSF grant DMS-0604382.

REFERENCES

[1] M. A. Hulsen, A. P. G. van Heel, B. H. A. A. van den Brule, *Simulation of viscoelastic flows using Brownian configuration fields*, J. Non-Newtonian Fluid Mech. 70, 79–101, 1997

[2] W. Ren, W. E, *Heterogeneous multiscale method for the modeling of complex fluids and microfluidics*, J. Comp. Phys. 204, 1–26, 2005.

[3] W. E, J. Lu, *Seamless multiscale modeling via dynamics on fiber bundles*, Commun. Math. Sci. 5, 649-663, 2007

[4] J. H. Irving, J. G. Kirkwood, *The statistical mechanical theory of transport processes IV*, J. Chem. Phys. 18, 817–829, 1950

[5] A. J. Chorin, *A numerical method for solving incompressible viscous flow problems*, J. Comp. Phys. 2, 12-26, 1967

[6] R. Car, M. Parrinello, *Unified approach for molecular dynamics and density functional theory*, Phys. Rev. Lett. 55, 2471–2474, 1985

[7] E. Vanden-Eijnden, *On HMM-like integrators and projective integration methods for systems with multiple time scales*, Commun. Math. Sci. 5, 495–505, 2007

[8] W. E, W. Ren, E. Vanden-Eijnden, *Remarks on seamless algorithms for problems with multiple time scales*, in preparation

[9] M. P. Allen, D. J. Tildesley, *Computer simulation of Liquids*, Oxford Science Publications, 1987.

[10] C. J. García-Cervera, W. Ren, J. Lu, W. E, *Sequential multiscale modeling using sparse representation*, draft

[11] B. D. Todd, P. J. Daivis, *Nonequilibrium molecular dynamics simulations of planar elongational flow with spatially and temporally periodic boundary conditions*, Phys. Rev. Lett. 81, 1118–1121, 1998

[12] A. Baranyai, P. T. Cummings, *Steady state simulation of planar elongational flow by nonequilibrium molecular dynamics*, J. Chem. Phys. 110, 42–45, 1999

[13] I. Fatkullin, E. Vanden-Eijnden, *A computational strategy for multiscale systems with applications to Lorenz 96 model*, J. Comp. Phys. **200**, 605–638 (2004)